PROCEEDINGS OF SCIENCE

Electromagnetic Dissociation at Cosmic-ray Energies

Ralph Engel,[a,c,*] **Anatoli Fedynitch,**[d] **Alfredo Ferrari,**[a,b,*] **Mario N. Mazziotta,**[e] **Tanguy Pierog,**[a] **Paola R. Sala**[f] **and Michael Unger**[a]

[a] *Karlsruhe Institute of Technology KIT, Institute for Astroparticle Physics, Germany*
[b] *Karlsruhe Institute of Technology KIT, Institute for Beam Physics and Technology, Germany*
[c] *Karlsruhe Institute of Technology KIT, Institute of Experimental Particle Physics, Germany*
[d] *Institute of Physics, Academia Sinica, Taipei City, 11529 Taiwan*
[e] *Istituto Nazionale di Fisica Nucleare, Sezione di Bari, I-70125 Bari, Italy*
[f] *The FLUKA Association, Thoiry, 01710 France*

E-mail: ralph.engel@kit.edu,alfredo.ferrari@kit.edu

Electromagnetic dissociation (EMD) is a well-known process that has been extensively studied using accelerator beams. However, the influence of EMD on cosmic-ray propagation in the atmosphere and galaxy remains unclear. For instance, understanding the origin of ultra-high energy cosmic rays requires knowledge of their mass composition. This can be determined by measuring the depth of the maximum of air shower development (X_{max}) and, in particular, the fluctuations of showers around their mean. Due to its substantial cross section, EMD could modify these observables, especially for heavy nuclei. This paper presents reliable predictions of cross sections, particle yields, and nuclear fragments produced in electromagnetic dissociation interactions at cosmic-ray energies for various projectiles on air. A brief description of the model for predicting EMD cross sections and subsequent (virtual) photon interactions is provided. This model is embedded in the FLUKA code, has been validated, and has been used at energies ranging from a few GeV/n to LHC energies. Recently, the virtual and real photon interaction models in FLUKA have been significantly improved; a brief description of these changes is included. The impact of EMD interactions on cosmic-ray showers in the atmosphere is shown to be minimal. At the same time, FLUKA's sophisticated photonuclear models have also been applied to explore their suitability for extragalactic cosmic ray propagation studies. A preliminary calculation of the energy loss length, considering the cosmic microwave background (CMB) and extragalactic background light (EBL) radiation fields, is presented for several ions ranging from protons to uranium.

39th International Cosmic Ray Conference (ICRC2025)
15–24 July 2025
Geneva, Switzerland

*Speaker

PoS(ICRC2025)252

1. Introduction

Many astrophysical environments are characterized by abundant background fields of photons providing an important scattering target for high-energy particles. In addition to electromagnetic processes, which are well understood within QED, photo-hadronic processes are of direct relevance. The same type of photo-hadronic interactions occur in interactions of hadrons with nuclei, where the virtual photon field of the nucleus provides the target. Therefore the understanding and detailed simulation of photo-hadronic interaction rates and the production of the corresponding secondary particles are very important for the interpretation of astrophysical observations.

The numerical simulation of these processes, which are currently not calculable from first principles, requires the combination of dedicated models and measurements of a multitude of different interaction channels. This has been done within the FLUKA simulation package, which has been extensively optimized and tested with a large set of data. After giving an introduction and short overview of FLUKA, we will use it in this work to make predictions for two kinds of photo-hadronic processes, (i) electromagnetic dissociation of primary cosmic rays entering the Earth atmosphere, prior to undergoing hadronic scattering and multiparticle production, and (ii) interaction and disintegration of nuclei propagating through the background photon fields of the Universe.

2. FLUKA and photonuclear interactions

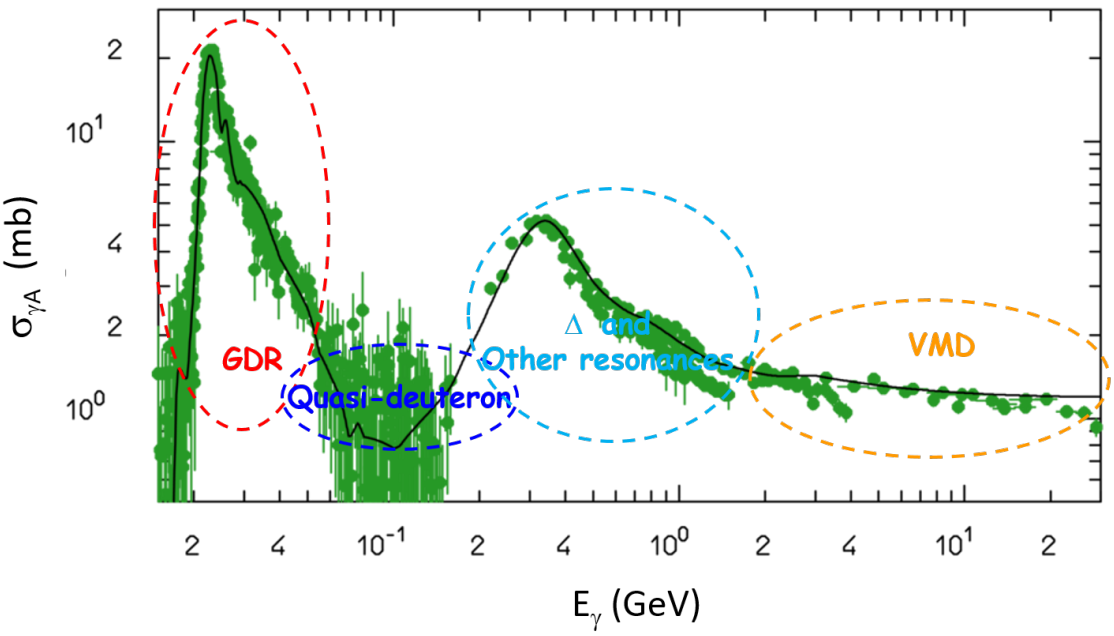

Figure 1: The FLUKA γC cross section from threshold up to 30 GeV (black line). Experimental data from various sources [1] and [2–5] are superimposed (green symbols).

The FLUKA Monte Carlo is a multi-purpose radiation transport and interaction code package, which is widely used to simulate particle-matter interactions in various fields, including high-energy

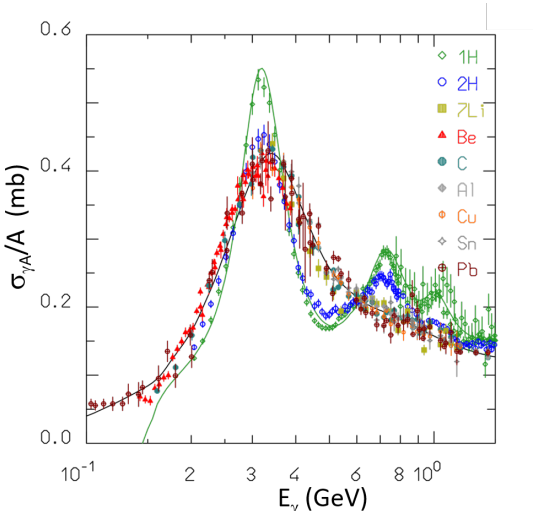

Figure 2: The FLUKA universal curve (black) for γ-nucleus interactions in the Δ region and beyond. Experimental data [1] for $\sigma(\gamma A)/A$ for various nuclei are superimposed. The adopted curve (green) for γp is also shown, in order to show the different width and peak value for nuclear targets.

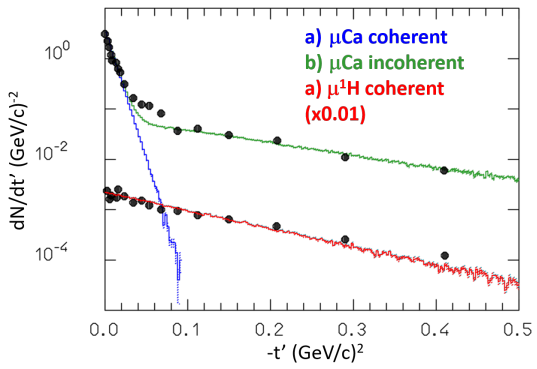

Figure 3: FLUKA computed $^{1}\mathrm{H}(\mu,\rho^{0})$ and $^{40}\mathrm{Ca}(\mu,\rho^{0})$ cross sections for 470 GeV/c muons are presented as a function of the 4-momentum transfer. The blue line represents the VMD coherent contribution, the green one the VMD quasi-elastic (incoherent) contribution, both on Ca. The red line is the coherent contribution on H. The symbols are exp. data from [6] with an arbitrary common normalization factor.

Table 1: One side only EMD cross section (with at least one neutron), and fractions (in %) of EMD events with given numbers of neutrons but without neutrons on the opposite side, for Pb-Pb collisions at $\sqrt{s_{\mathrm{NN}}}$=2.76, 5.02 TeV. Exp. data from [7, 8] .

	$\sqrt{s_{\mathrm{NN}}}$			
	2.76 TeV		5.02 TeV	
	Exp.	FLUKA	Exp.	FLUKA
$\sigma_{\mathrm{EMD\ xn}}$ (b)	$181.3\pm 0.3^{+12.8}_{-10.9}$	181.9± 0.1	–	204.4 ± 0.1
$N_{1n}/N_{\mathrm{one-side}}$ (%)	51.5±0.4±0.2	50.6±0.1	52.4 ±0.2 ±1.3	48.9±0.1
$N_{2n}/N_{\mathrm{one-side}}$ (%)	11.6±0.4±0.5	11.6±0.1	11.94±0.03±0.563	11.5±0.1
$N_{3n}/N_{\mathrm{one-side}}$ (%)	3.6±0.2±0.2	3.0±0.1	3.74±0.02±0.07	3.1±0.1
$N_{4n}/N_{\mathrm{one-side}}$ (%)	–	2.3±0.1	2.66±0.01±0.14	2.3±0.1

physics, space radiation, and medical applications, radiation protection, and accelerator studies, and astrophysics. The modern version of FLUKA, as used in this work, goes back to work started in 1989 at INFN-Milan by A. Ferrari and P. Sala, with important contributions from A. Fassò and J. Ranft. A detailed history of FLUKA can be found in Ref. [9, 10].

2.1 Real photons

Figure 1 shows the FLUKA photonuclear cross sections for carbon over the entire energy range, from the threshold to several tens of GeV. As indicated, the cross section spans four different regimes transitioning from the Giant Dipole Resonance (GDR) into inelastic regimes above the pion production threshold. The FLUKA photonuclear interaction models were initially developed

in the 1990s (see references [11, 12]). Today, new data and a deeper theoretical understanding enable a more complete and accurate description of photonuclear interactions, both real and virtual. In recent years, therefore, the FLUKA photonuclear cross sections and interaction algorithms have been extensively revised, with particular attention paid to the quasi-deuteron (QD) and the transition to the Vector Meson Dominance (VMD) model energy ranges. The (Δ) resonance region is modeled using a data-driven technique (see Fig. 2). Additionally, the GDR cross sections for all light nuclei and some heavy nuclei have been updated. FLUKA contains a total of 190 isotope-specific tabulated GDR data sets. For other isotopes, up-to-date parameterizations are used. Examples of the new photonuclear interaction cross sections can be found in Ref. [10].

2.2 Virtual photons

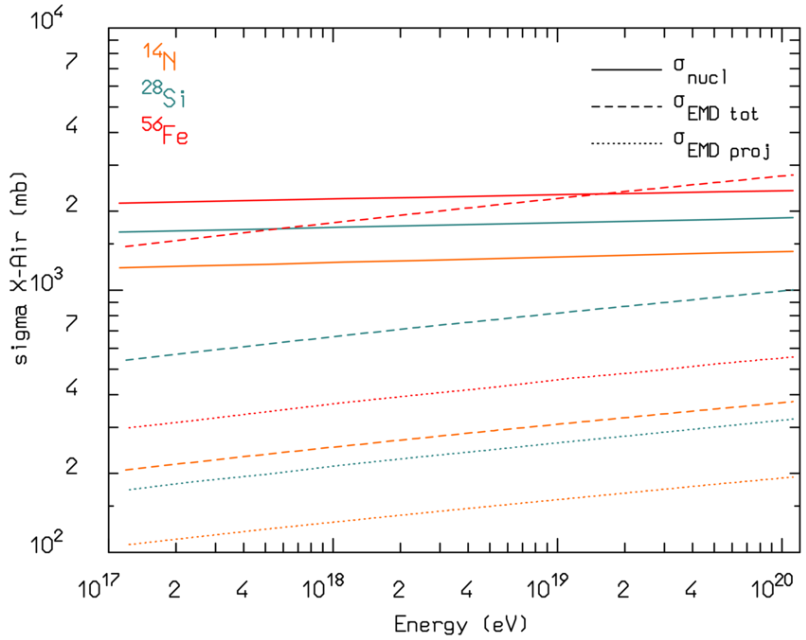

Figure 4: The computed nuclear and EMD cross sections in air for ^{14}N, ^{28}Si and ^{56}Fe as a function of total energy. Solid curves are the nuclear cross sections, dashed curves the EMD cross section, the dotted curves the EMD projectile-dissociation one.

The EMD model in FLUKA has already been validated against a variety of experimental data and applied at LHC energies with promising results [13]. Over the years, the model has been improved [14] to include the E2 multipolarity, nuclear finite size and higher-order effects, all of which are important at low energies and for $e^{\pm}$ and μ. FLUKA EMD has been extended to handle muon-nuclear interactions below the $\gamma + N \rightarrow \pi + X$ threshold, and can simulate electro-nuclear interactions. The same formalism also applies to deuteron Coulomb dissociation as well. The EMD cross section is expressed as a sum over multipolarity i of the convolution of the number of emitted (virtual) photons, n_i, with the photon-nucleus cross section $\sigma_{i\,\gamma A}$

$$\sigma_{\mathrm{EMD}} \approx \sum_i \int_{E_{\mathrm{min}}}^{E_{\mathrm{max}}} \sigma_{i\,\gamma A}\left(E_\gamma\right) n_i\left(E_\gamma\right) \frac{\mathrm{d}E_\gamma}{E_\gamma}. \tag{1}$$

Table 2: Average X_{max} and its RMS for 3 different ions at 4 different total energies, with and without electromagnetic dissociation (EMD).

Projectile	Energy (eV)	<X_{max}>		RMS	
		EMD (g cm^{-2})	No EMD (g cm^{-2})	EMD (g cm^{-2})	No EMD (g cm^{-2})
^{56}Fe	$5.6 \cdot 10^{18}$	712.5 ± 0.3	712.6 ± 0.3	20.55 ± 0.19	20.62 ± 0.18
^{56}Fe	$5.6 \cdot 10^{19}$	779.2 ± 0.3	779.2 ± 0.3	18.88 ± 0.18	19.41 ± 0.18
^{14}N	$2.8 \cdot 10^{19}$	799.1 ± 0.4	799.3 ± 0.4	29.32 ± 0.28	29.70 ± 0.26
^{28}Si	$1.12 \cdot 10^{20}$	819.2 ± 0.3	819.2 ± 0.3	22.42 ± 0.17	23.21 ± 0.20

It can be shown that the dominant components are E1 and E2. Since E2 is significant at low energies, and M1 is always negligible, equation 1 becomes

$$\sigma_{\mathrm{EMD}} \approx \int_{E_{\mathrm{min}}}^{E_{\mathrm{max}}} \left[\sigma_{E1\,\gamma A}\left(E_\gamma\right) n_{E1}\left(E_\gamma\right) + \sigma_{E2\,\gamma A}\left(E_\gamma\right) n_{E2}\left(E_\gamma\right)\right] \frac{\mathrm{d}E_\gamma}{E_\gamma}. \tag{2}$$

The E2 contribution is important in order to reproduce EMD data for ions at energies of a few hundreds MeV/n. For instance, FLUKA predicts that E2 accounts for 25% of the total EMD cross section for ^{238}U on ^{238}U at 120 MeV/n, a value in agreement with other theoretical predictions [15] and consistent with experimental total cross sections. Figure 3 compares the computed and experimental [6] production of the ρ_0 meson as a function of four-momentum transfer for 470-GeV/c positive muons impinging on targets of ^{40}Ca and ^{1}H. Table 1 shows a comparison of the FLUKA EMD model in its most recent formulation against data taken by the Alice experiment at the LHC concerning validation at the highest energies. These examples illustrate the ability of FLUKA to reproduce virtual photon-induced reactions.

3. Photo-disintegration in extensive air showers

Photodisintegration in air showers occurs in real-photon-air interactions and through virtual-photon exchange in peripheral collisions of air shower nuclei. Figure 4 shows the computed EMD air cross sections for three different ions. The figure displays both the total EMD cross section and the projectile dissociation component. Both are compared with the nuclear cross section.

To investigate the impact of EMD interactions, we carried out simulations with and without EMD using FLUKA coupled with DPMJET-III.19.3 [16, 17] for vertical showers in the standard US atmosphere.

Several projectile energy combinations were explored to determine the impact of considering EMD versus not considering it. In each case, 5,000–6,500 individual showers were simulated with suitable thinning parameters to minimize the impact on shower-to-shower fluctuations. A standard 6-parameter Gaisser-Hillas fit is applied to the longitudinal profile of the energy deposition to extract the position of the shower maximum. The results on the calculated average shower maximum and its rms are presented in Table 2. We have also compared the spectra of muons, neutrons, protons, photons, and electrons/positrons. Once the initial fluctuations due to the first interaction point are

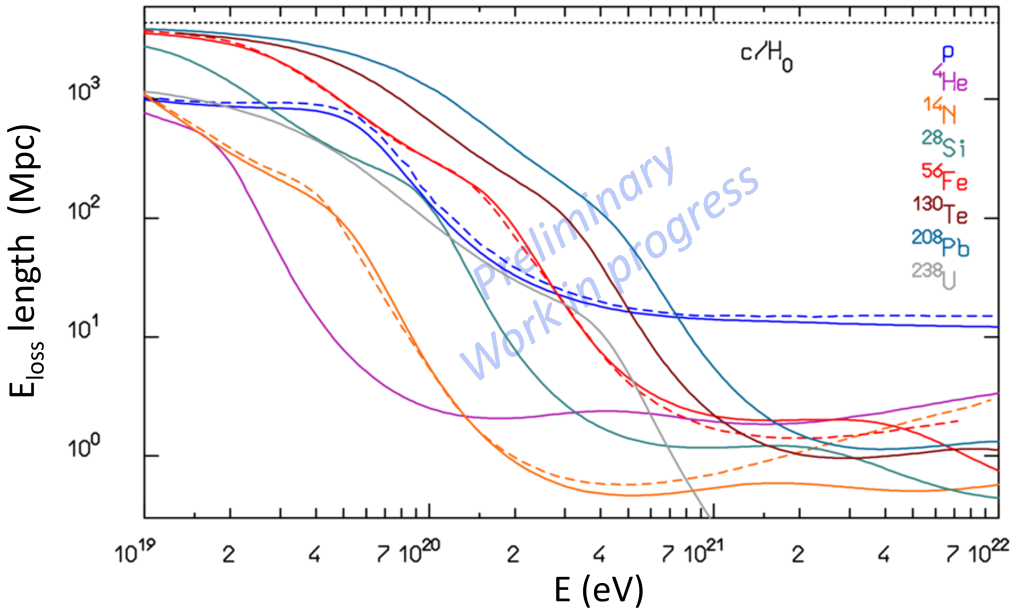

Figure 5: The computed energy loss lengths as a function of the total ion energy, assuming H_0=69 km/s/Mpc. The CMB and EBL spectra are accounted for, as well as the Bethe-Heitler pair production. The dashed lines are the results for ^{1}H ^{14}N and ^{56}Fe of Refs. [18, 19].

averaged out, no detectable differences can be found within the statistical errors (a fraction of a percent).

4. High energy cosmic ray propagation

We also investigated the propagation of light, medium, and heavy nuclei at ultrahigh-energy cosmic ray (UHECR) energies in the cosmic microwave background (CMB) and extragalactic background light (EBL) photon fields. The CMB spectrum was assumed to be a blackbody spectrum at T=2.725 K, while the EBL spectrum is from Ref. [20]. The impact of the disintegration model on UHECR propagation has been extensively studied in Ref. [21, 22] and more recently in Refs. [23, 24] and is shown to influence the inference of UHECR source parameters.

Our results are presented in Figures 5 and 6 as a function of the projectile's total energy and energy per nucleon, respectively. Due to the recent interest in UHECR's with masses heavier than iron [25, 26], we also show the results for ^{130}Te, ^{208}Pb, abd ^{238}U. For each combination of projectile energy, 300,000 Monte Carlo events were generated. The loss lengths were computed as $L_{\rm loss} = \lambda_{\rm mfp}^{\rm CMB\ EBL} \cdot \Delta E/E$, where ΔE is the energy loss between the original projectile and the heaviest secondary fragment. This approach is very fast and properly accounts for fluctuations event-by-event without requiring the generation of large databases. It also allows for a more realistic estimation of $L_{\rm loss}$ by tracking the secondary fragments and simulating their interactions. The comparison in energy per nucleon is particularly insightful, as it shows that apart from protons, which are affected only by photopion production, and to a lesser extent ^{4}He, all other ions exhibit the same behavior. Their spread stems from differences in GDR cross sections and reaction thresholds specific to individual isotopes. The only exception is ^{238}U, which can undergo photo-fission at

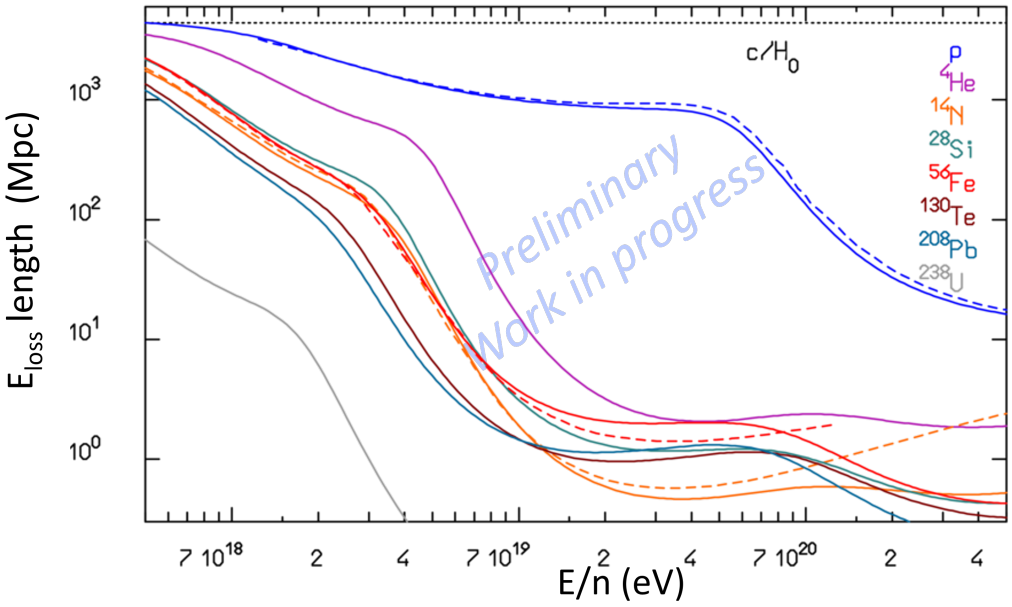

Figure 6: Same as in Figure 5, but plotted as a function of the energy per nucleon.

photon energies of a few MeV, suffering catastrophic energy losses at the first interaction. For comparison, the results of Ref. [19], based on CRpropa [27], for ^{14}N and ^{56}Fe and of Ref. [18] for ^{1}H are also shown. The results are generally consistent, except at the highest ion energies, where a proper description of gamma-nucleus interactions in the $\Delta(1232)$ region, including multinucleon interactions and nuclear deexcitation, yields strikingly different results than the extrapolation from gamma-nucleon photopion production. Indeed, the results of Ref. [28], which uses a model specific for gamma-nucleus in the Δ region (albeit less detailed than the FLUKA one), are more similar to ours.

Conclusions

FLUKA, in combination with DPMJET-III.19.3, was used to assess the impact of electromagnetic dissociation (EMD) on ultra-high-energy cosmic-ray (UHECR) air showers. Although the EMD cross section constitutes a sizable fraction of the total nuclear cross section, no statistically significant differences were observed in key shower observables, such as $X_{\max}$, energy deposition, or the longitudinal and radial profiles of particle fluxes, when EMD was enabled. Only at the highest energies tested does a slight reduction in the $X_{\max}$ RMS become noticeable.

As a further application of the photonuclear interaction modeling in the state-of-the-art FLUKA framework, we have calculated the UHECR interaction rate and energy loss length due to interactions with the CMB and EBL photon fields. The results are compared with those from the widely used CRpropa implementation, showing good agreement across the most relevant energy range. However, unlike existing simulation packages, FLUKA enables detailed modeling of these processes for a much broader range of nuclei, including heavy species beyond iron, as demonstrated in this work.

Acknowledgements AF acknowledges support from the Academia Sinica (Grant No. AS-GCS-113-M04) and the National Science and Technology Council (Grant No. 113-2112-M-001-060-MY3).

References

[1] "Experimental Nuclear Reaction Data (EXFOR)." [Online]. Available: https://www-nds.iaea.org/exfor

[2] D. O. Caldwell, V. B. Elings, W. P. Hesse, R. J. Morrison, F. V. Murphy, and D. E. Yount, *Phys. Rev. D*, vol. 7, p. 1362, 1973.

[3] G. R. Brookes *et al.*, *Phys. Rev. D*, vol. 8, pp. 2826–2836, 1973.

[4] S. Michalowski, D. Andrews, J. Eickmeyer, T. Gentile *et al.*, *Phys. Rev. Lett.*, vol. 39, pp. 737–740, 1977.

[5] E. Arakelyan, G. Bayatyan, G. Vartanyan, N. Grigoryan *et al.*, *Physics Letters B*, vol. 79, no. 1, pp. 143–146, 1978.

[6] M. R. Adams, S. Aïd, P. L. Anthony, D. A. Averill *et al.*, *Phys. Rev. Lett.*, vol. 74, pp. 1525–1529, 1995.

[7] B. Abelev, J. Adam, D. Adamová, A. M. Adare *et al.*, *Phys. Rev. Lett.*, vol. 109, p. 252302, Dec 2012.

[8] S. Acharya, D. Adamová, A. Adler, G. Aglieri Rinella *et al.*, *Phys. Rev. C*, vol. 107, p. 064902, 2023.

[9] A. Ferrari, P. R. Sala, A. Fassò, and J. Ranft, "FLUKA: A multi-particle transport code (Program version 2005)," CERN INFN SLAC, Tech. Rep. CERN-2005-010, SLAC-R-773, INFN-TC-05-11, CERN-2005-10, 10 2005. [Online]. Available: https://doi.org/10.2172/877507

[10] F. Ballarini, K. Batkov, G. Battistoni, M. G. Bisogni *et al.*, *EPJ Nuclear Sciences & Technologies*, vol. 10, p. 16, 2024, publisher: EDP Sciences.

[11] A. Fassò, A. Ferrari, and P. R. Sala, in *Radiation shielding, International Conference on Radiation Shielding*, vol. 2. La Grange Park: American Nuclear Society;, 1994, pp. 643–649.

[12] A. Fassò, A. Ferrari, and P. R. Sala, in *Proc. 3rd Specialists' Meeting on Shielding Aspects of Accelerators, Targets and Irradiation Facilities*, 1997, p. 61.

[13] H. H. Braun, A. Fassò, A. Ferrari, J. M. Jowett, P. R. Sala, and G. I. Smirnov, *Phys. Rev. ST Accel. Beams*, vol. 17, no. 2, p. 021006, 2014.

[14] F. Cerutti, A. Empl, A. Fedynitch, A. Ferrari *et al.*, *EPJ Web Conf.*, vol. 146, p. 12005, 2017.

[15] M. L. Justice, Y. Blumenfeld, N. Colonna, D. N. Delis *et al.*, *Phys. Rev. C*, vol. 49, pp. R5–R9, 1994.

[16] A. Fedynitch and R. Engel, in *14th International Conference on Nuclear Reaction Mechanisms*, Varenna, Italy, June 2015, p. 291.

[17] A. Fedynitch, https://github.com/DPMJET/.

[18] T. Stanev, R. Engel, A. Mücke, R. J. Protheroe, and J. P. Rachen, *Phys. Rev. D*, vol. 62, p. 093005, 2000.

[19] R. A. Batista, D. Boncioli, A. di Matteo, A. v. Vliet, and D. Walz, *Journal of Cosmology and Astroparticle Physics*, vol. 2015, no. 10, p. 063, oct 2015.

[20] R. C. Gilmore, R. S. Somerville, J. R. Primack, and A. Domínguez, *Monthly Notices of the Royal Astronomical Society*, vol. 422, no. 4, pp. 3189–3207, 05 2012.

[21] J. Heinze, A. Fedynitch, D. Boncioli, and W. Winter, *Astrophys. J.*, vol. 873, no. 1, p. 88, 2019.

[22] L. Morejon, A. Fedynitch, D. Boncioli, D. Biehl, and W. Winter, *JCAP*, vol. 11, p. 007, 2019.

[23] E. Kido, T. Inakura, M. Kimura, N. Kobayashi *et al.*, *Astropart. Phys.*, vol. 152, p. 102866, 2023.

[24] A. Tamii *et al.*, *Eur. Phys. J. A*, vol. 59, no. 9, p. 208, 2023.

[25] B. T. Zhang, K. Murase, N. Ekanger, M. Bhattacharya, and S. Horiuchi, "Ultraheavy ultrahigh-energy cosmic rays," 2024. [Online]. Available: https://arxiv.org/abs/2405.17409

[26] G. R. Farrar, *Phys. Rev. Lett.*, vol. 134, p. 081003, 2025.

[27] R. Alves Batista, A. Dundovic, M. Erdmann, K.-H. Kampert *et al.*, *JCAP*, vol. 05, p. 038, 2016.

[28] D. Allard, *Astroparticle Physics*, vol. 39-40, pp. 33–43, 2012, Cosmic Rays Topical Issue.

PoS(ICRC2025)252